Materials and Nanotechnology

Glass matrices to contain industrial and radioactive wastes

Materials and Nanotechnology

Introduction

The focus of the Materials and Nanotechnology Program is technology development related to processing, analysis, testing and characterization of materials in general. These are achieved through execution of R&D projects in engineering and materials science, cooperative projects with private and public sector companies, universities and other research institutes. Besides technology development, this Program also fosters training and human resource development in association with the University of São Paulo and many industrial sectors. This Program is divided into sub-programs in broad areas such as ceramic, composite and metallic materials as well as characterization of physical and chemical properties of materials. The sub-programs are further divided into general topics and within each topic, R&D projects.

Ongoing work in the ceramic materials area consists of R&D projects on biomaterials and this includes bio-inert, bio-active or re-absorbable ceramics and new biomedical alloys. Glasses are being developed to immobilize nuclear wastes and to produce microspheres for radiotherapy treatment. Activities related to solid oxide fuel cells are synthesis, processing and production of appropriate materials and testing of unit cells. Advanced ceramic materials with tailored microstructures for specific applications include those based on silicon nitride, silicon carbide, zirconia and alumina. In the area of metallic materials, the activities include development of: (a) sintered components for use as cutting tools; (b) solid hydrogen storage materials based on TiFe intermetallic compounds; (c) batteries and magnets using the hydrogen decrepitation process and the powder metallurgy route. The activities related to Physical and Chemical property characterization were development of: (a) nanostructured coatings of Cr_3C_2-Ni20Cr and WC-Co for increased H.T. degradation resistance; (b) rare earth oxide gel coatings for chromia and alumina forming alloys; (c) nanocrystalline metal-organic chemical vapor deposited films of TiO_2/TiNO, CrN and CrO; (d) self-organized monolayer (SAM) coatings for steel and aluminum alloy automotive components; (e) coated stainless steels and Ti alloys for use as implants; (f) corrosion inhibitors for carbon steels for use as reinforcement in concrete structures. Efforts in terms of materials and technologies development for a sustainable environment were focused on mitigation of environmental impact of solid wastes, increase in energy efficiency, use of green technologies to reuse debris and wastes to produce glass-silicate fibers. A high-pressure cell for use at the Brazilian Synchrotron Light Laboratory and in the IPEN neutron diffractometer has been developed. A carbon and glass fiber composite pipe was constructed for use as lower limb prosthesis to optimize cost and reduce weight. Magnetics hydrogels are being developed for biomedical applications, such as treatment of burns and controlled drug delivery.

Biomedical alloys

Endosseous implant studies in the biomedical area using titanium alloy Ti13Nb13Zr has as its objective the resolution of lifetime related problems in organisms. These studies consist of production of porous metallic biomaterials using powder metallurgical techniques with additives such as gelatin, alginate, starches and albumin, either dry or as a suspension. The titanium substrate with a structurally graded interface and the molecular profile of tissue response with the implant in place were also investigated (Figure 1). The observed structures in the presence of these molecules in the tissue, improved understanding and manage setbacks faced during tissue repair involving implants.

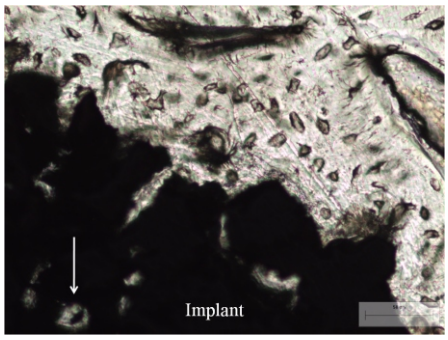

Figure 1. Bone-implant interface. Bright field shows histological slide without staining in which the dark area represents the porous metallic implant. The white arrow indicates the osteocyte inside a pore.

Bioceramics

Calcium phosphate based ceramics, especially tricalcium phosphate and hydroxyapatite, are considered promising materials for bone reconstitution and substitution due to its composition. Calcium phosphate ceramics were obtained in the macroporous form by the direct consolidation method using albumin. The filling of the macropores with new bone tissue resulted in strong interlaced bone-implant and conferred increased strength to the implant (Fig. 2a). This fact is expected to promote cell differentiations and bone formation. Fig. 2b reveals the biphasic ceramic implant (dark region) being invaded by newly formed bone (violet region).

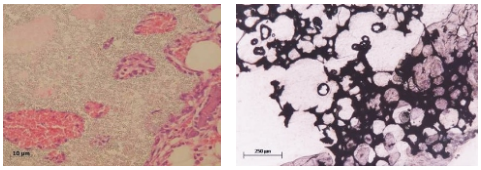

(a) (b)

Figure 2. Histological analysis: (a) osseointegration process in decalcified slide (after 1 week); (b) general view of in-growth of bone, calcified slide (after 4 weeks). (Hematoxilin -Eosin staining)

Properties related to biocompatibility of mixed ceramics ZrO_2-TiO_2 prepared with different rates content were compared by analysis of cultured FMM1 fibroblasts. The specimens were plated on top of disks and counted in SEM micrographs and subsequently analyzed after 1 and 2 days. The cell growth on ZrO_2-TiO_2 samples was similar and significantly higher than those on TiO_2 or ZrO_2 samples. The in vitro experiments showed that sintered ZrO_2-TiO_2 ceramics were biocompatible permitting faster cell growth compared with pure oxide ceramics. Thus, the ZrO_2-TiO_2 sintered ceramics can be considered as a potential implant material.

Silicon nitride based ceramics are promising candidates for biomedical applications due to their chemical and dimensional stability along with adequate mechanical strength and relatively high fracture toughness. The sintered specimens containing La_2O_3 and Al_2O_3 additions had densities higher than 94% of the theoretical density. The bioinert characteristics of silicon nitride ceramics limit its use where the formation of chemical bonds between the material and the tissue are not essential. Samples of silicon nitride were coated with apatite using the biomimetic method. The layer of hydroxyapatite could be deposited by this method on silicon nitride samples surface.

Dental Ceramics

The development of alumina and zirconia based materials, which exhibit aesthetic properties, biocompatibility and good mechanical behavior, enables its use for dental restorations. The incorporation of a vitreous phase in these ceramics is an alternative to minimize ceramic retraction during sintering, besides improving adhesion to resinbased cements, aspects essential to bind dental frameworks to the porcelain cover. Zirconia and alumina based powders were synthesized by the hydroxide coprecipitation route and incorporation of the vitreous phase was done by impregnation of aluminum borosilicate lanthanum powder in sintered ceramics, Fig. 3. Synthesized powders resulted in ceramics with fracture toughness in the range 3.6 - 6.0 $MPa.m^{1/2}$, (comparable to commercially reinforced ceramic materials) and with no citotoxic effects. Bond durability studies between zirconia ceramic and the phosphate resin cement after surface conditioning have been also carried out.

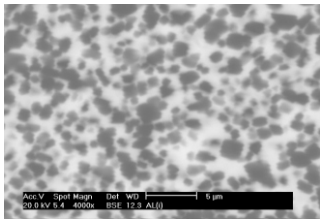

Figure 3. SEM micrograph of alumina ceramic (gray phase) after aluminum-borosilicate lanthanum glass incorporation (white phase)

Ceramic Composites

Ceramic matrix composites have been used as potential materials in load bearing aggressive environments at high temperature. In this context, NbC, TaC and TiC were used as second phase in alumina ceramics to manufacture ceramic nanocomposites for high performance cutting tools. Microcomposites with homogeneous microstructures were produced by adding 1,.5 vol.% NbC, TaC and TiC to the alumina matrix processed by pressure sintering at 1500°C/30min and 20MPa. Nanocomposites Alumina matrix composites with nanometric NbC particles were synthesized by reactive high energy milling with the addition of commercial SiC, ZrO_2 and diamond and studied. The tests simulating thermodynamic conditions of cutting a diffusion pair with gray cast iron were carried out and the composites exhibited good chemical stability upon contact with metal under high pressure and temperature. Based in these results, ceramic cutting tool samples (size 15x15 mm) were prepared and rectified to achieve the geometry of a standard cutting tool to evaluate during machining of hard metals, Figure 4.

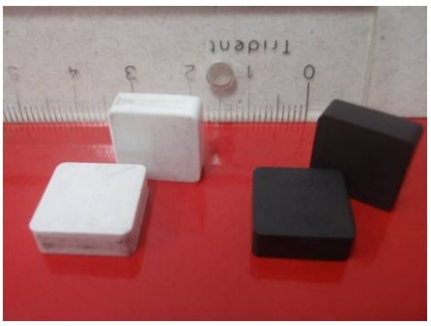

Figure 4. Ceramic cutting tool produced with alumina matrix composites

Ceramic Composites with inorganic polymers additions

Alumina and silicon carbide based composites with polymeric precursors were developed and characterized. Alumina composites were obtained with the addition of active fillers, metallic Ti with two different particle size distributions. These had a homogeneous microstructure and revealed the refractory phases, mullite and TiCN. The preparation of ceramic composites using small amounts of precursor polymers is a simple forming route, with high potential for the production of complex shaped pieces.

Covalent ceramics

Statistical mixture designs are used to systematically study the densification properties of silicon carbide (SiC) ceramics sintered with SiO_2, Dy_2O_3, and Al_2O_3. Mixture models for specific percentage theoretical density and SiC weight loss as a function of the SiO_2, Dy_2O_3, and Al_2O_3 oxide proportions have been determined and validated by analysis of variance. The results indicate a region confined by about 0-20mol% silica, 50-65 mol% dysprosia, and 40-65mol% alumina, with all samples containing 10 vol % of additives, and simultaneous maximization of densities and minimization of weight loss during SiC-based ceramic sintering. Porous structural ceramics based on covalent materials (SiC and Si_3N_4) have been developed, using gelcasting and sacrificial template with different types of starch (rice, potato and corn) as pore forming and consolidation agents. Gelcasting provided porous ceramic samples with the best mechanical properties, where the values obtained were higher than other porous ceramics used commercially, such as alumina and mullite. The porosity of the samples ranged between 25 and 37% and mechanical strength between 100MPa and 240MPa.

The ceramic research group achieved national and international recognition, as shown on the cover of the American Ceramic Bulletin, Fig. 5.

Figure 5. Page in the American Ceramic Bulletin, September 2009

The production of ceramics with special mechanical, electrical, chemical and biological properties involves control of powder characteristics such as chemical composition, crystal structure, particle size, particle morphology, specific surface area and state of agglomeration. In this context, various chemical techniques have been studied at IPEN, to synthesize powders for fuel cell components and biomaterials. Co-precipitation of metal salts followed by hydrothermal and solvothermal treatments, as well as combustion synthesis are the processing routes that were used to synthesize stabilized zirconia, alumina, titania, samaria and gadolinia doped ceria and hydroxyapatite based nanosized powders. Forming processes such as pressing, tape casting and electrophoretic deposition followed by microwave sintering were used.

One of the main outcome are the micrographs of titania nanotubes, prepared by commercial titanium dioxide treatment in sodium solution in a pressured reactor (hydrothermal synthesis), as shown in Figure 6. Among the different oxide nanotubes, worthy of mention is titania, due to its strong oxidizing power, chemical inertness, non-toxicity and unique functional properties that are relevant in terms of applications: photovoltaic cells, gas sensing, photocatalysis, selective adsorption and pollutant elimination. Quite recently, the use of titania nanotubes-based materials has been extended to drug release, based on its excellent biocompatibility and easy surface modification. Hydrothermal synthesis is also a good alternative to synthesize nanocrystalline powders at temperatures as low as 200°C, eliminating thus the calcination step. A TEM micrograph of zirconia powder prepared by this method is shown in Figure 7.

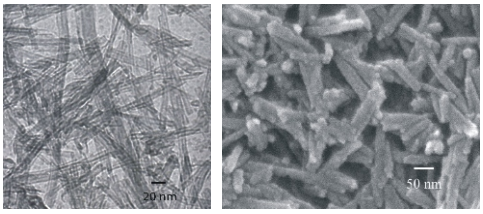

Figure 6. Micrographs obtained by transmission electron microscopy (TEM) and field-emission scanning electron microscopy (FE-SEM) of titania nanotubes

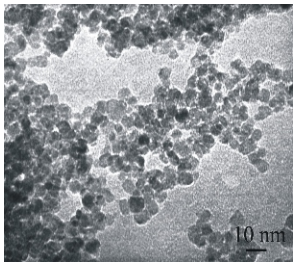

Figure 7. Micrograph obtained by transmission electron microscopy (TEM) of hydrothermally treated stabilized zirconia powders

High temperature degradation resistant coatings

A variety of single rare earth oxide coatings have been developed to improve high temperature oxidation resistance of chromium dioxide and alumina forming alloys. Further increase in high temperature oxidation resistance of these alloys was achieved through optimization of the role of specific rare earths and the use of mixed rare earth oxide coatings.

Corrosion resistant coatings

Cerium based coatings. Cerium based conversion coatings, cerium impregnated boehmite coatings and hydrotalcite coatings were developed to increase the aqueous corrosion resistance of aluminum alloys and specially to protect spent aluminum-clad research reactor fuels during long term wet storage. Hydrotalcite coatings (Fig. 8) modified with cerium was the most efficient coating.

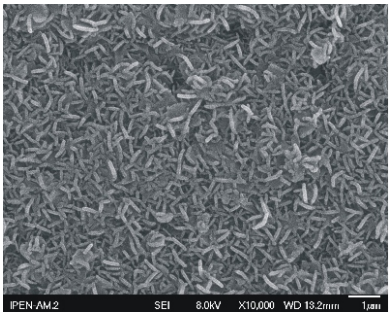

Figure 8. Hydrotalcite layer on aluminum alloy AA 6061 surface

Chromium-free coatings for aluminum alloys

The protective properties provided by various surface treatments to aluminum were evaluated with the aim of replacing coatings based on hexavalent chromium, considered harmful to the environment and to human health. Various treatments that were given to AA 1050 to increase its corrosion resistance were investigated, and included, treatment with self assembling molecules based on diphosphonates (SAM), immersion in boiling water for oxide growth (bohemitization), combination of the two treatments in the sequence (Bohemitization+SAM), passivation in trivalent chromium solution and passivation in hexavalent chromium solution. The corrosion resistance of the various surface treatments was evaluated using techniques, such as salt spray testing according to ASTM B-117, electrochemical measurements and scanning electron microscopy. The results showed that the treatment with self assembling molecules did not protect the AA1050 aluminum for long periods of exposure to NaCl. The SAM treatment after bohemitization produced a surface layer with improved corrosion resistance and showed the importance of an oxy-hydroxide surface layer for adsorption of self-assembling molecules (OS). The passivation treatment based on trivalent chromium led to a surface with corrosion resistance similar to that based on hexavalent chromium. This indicated that the former is a viable alternative to replace hexavalent chromium. Fig. 9 shows the untreated and treated AA 1050 surfaces, prior to and after the salt spray test.

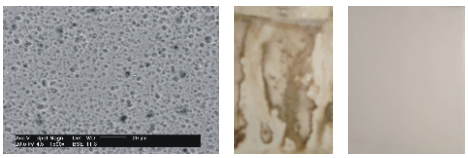

(a) (b) (c)

Figure 9. AA1050 surface (a) with bohemitization followed by SAM treatment; (b) without surface treatment after 148h of salt spray test, and (c) with bohemitization followed by SAM treatment after 148h of salt spray test

Corrosion behavior of biomaterials

Coatings produced by physical vapor deposition (PVD) methods have been applied to 316L stainless steel surfaces to increase its corrosion resistance and biocompatibility. Three thin films were tested: titanium nitride (TiN), titanium carbonitride (TiCN) and diamond-like carbon (DLC). These materials have high hardness, wear resistance and intrinsic biocompatibility, which are key features for biomedical applications. Characterization of the electrochemical behavior of stainless steel coated with the three different films revealed surface defects that decrease the corrosion resistance of the substrate. These PVD coats were non-cytotoxic and had high wear resistance. These properties along with the low cost of stainless steel make coated stainless steel a potential material for biomedical implants. However its corrosion resistance requires further improvement. Fig. 10 shows the DLC coated AISI 316 L stainless steel surface and cross section.

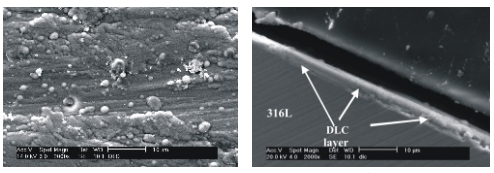

(a) (b)

Figure 10. Surface of AISI 316L stainless steel with DLC coating. (a) top and (b) cross-section.

Surface treatments to protect carbon steels

The viability of replacing nickel in zinc phosphate (PZn) baths with niobates, ammonium niobium oxalate and benzotriazole (BTAH), for phosphating of carbon steels, has been investigated. The effect of ammonium niobium oxalate as a passivant of phosphated steels was also evaluated. The phosphate layer formed in the PZn+Ni solution

consisted of needle like crystals, while that formed in PZn+Nb and PZn+Ox+BTAH solutions consisted of crystal-like grains with improved surface coverage. The phosphate layers obtained in the PZn+Nb and PZn+Ox+BTAH baths were thicker and rougher than the PZn+Ni layer favoring corrosion protection and coating adhesion. The PZn+Nb and PZn+Ox+BTAH layers were also less porous and more corrosion resistant, compared with PZn+Ni. These results helped conclude that Nb could replace Ni in phosphating baths. Fig. 11 shows the zinc phosphate coating from baths containing Ni and Nb.

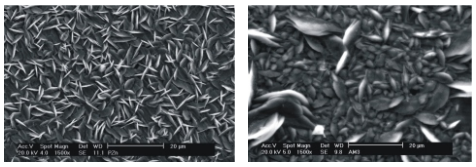

(a) PZn+Ni (b) PZn+Nb

Figure 11. Zinc phosphate coating obtained in (a) Ni and (b) Nb phosphating containing baths showing different morphologies of phosphate crystals

Electroceramics

Basic research work is devoted to the study of zirconia/ceria based ionic conductors and cerate/zirconate based protonic conductors, particularly for the development of solid oxide fuel cells and oxygen sensors. The synthesis of ceramic nanopowders is carried out by several techniques: coprecipitation, polymeric precursors, combustion and polyacrylamide. The characterization of the powders is carried out by in situ high temperature x-ray diffraction, thermal analysis and Fourier transform infrared absorption spectroscopy. Ceramic pieces are prepared by pressing and sintering. Conventional as well as fast firing and two-step sintering procedures are performed to obtain electroceramics with improved electrical behavior. Electrical measurements consist of impedance spectroscopy measurements in a wide temperature range (LNT-1500K) and oxygen partial pressures (10 ppm - 1 atm). Microstructure evaluations were carried out using x-ray diffraction analysis, scanning and transmission electron microscopy, scanning probe microscopy and Raman spectroscopy.

Soft chemistry techniques have been used to synthesize several oxygen-ion conductors with the aim of improving their microstructure and electrical properties. Pure and Gd-doped $La_2Mo_2O_9$ powders and films were prepared by the polymeric precursor technique. Gadolinium doping was efficient to stabilize the β-$La_2Mo_2O_9$ phase. Homogeneous and crack-free films were obtained using glass, alumina and silicon substrates. Nanostructured and single-phase tetragonal zirconia was prepared by the spray pyrolysis technique (Fig. 12).

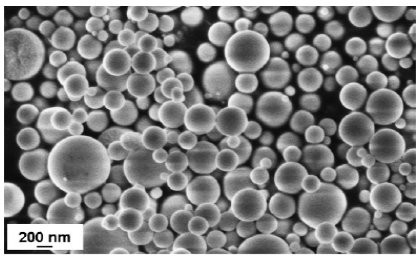

Figure 12. Scanning electron micrograph of tetragonal zirconia powder synthesized by spray pyrolysis

Thermal aging studies revealed that degradation is mainly related to chemical modifications at electrode/electrolyte interfaces and near the grain boundaries. Samaria-doped ceria nanoparticles were synthesized by homogeneous precipitation with hexamethylenetetramine. The as-prepared nanoparticles were crystalline and single-phase with fluorite-type structure (Fig. 13), and consisted of a mixture of anhydrous and hydrated cerium oxide with average size of 5-8 nm.

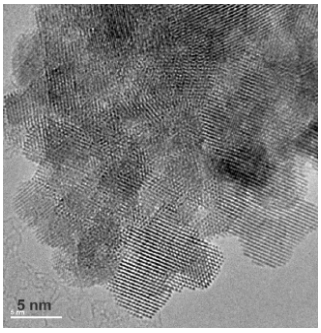

Figure 13. HRTEM micrograph of as-prepared samaria-doped ceria nanoparticles

Technological research work consists of operation of unitary solid oxide fuel cells with proton and oxide ion conductors in hydrogen, methane and ethanol atmospheres as well as the testing of oxygen lambda sensors. The main results were:

- Development and testing of anode-supported solid oxide fuel cells with slurry-coated electrolyte and cathode under ethanol and hydrogen;
- Characterization of sintered zirconia-yttria ceramics by impedance spectroscopy;
- Development of zirconia:magnesia-zirconia:yttria composites for high temperature oxygen sensors;
- Determination of the effect of additives on electrical performance of ceria-based materials;
- Synthesis of nanostructured zirconia and ceria-based solid electrolytes.

Glasses are being developed to immobilize industrial and nuclear wastes, to produce microspheres for radiotherapy treatments, and for optical, electrical, and mechanical applications. A mathematical model using the Monte Carlo method is being developed to determine the dose distribution in human liver when neutron active glass microspheres are directly injected in the organ through and artery. This is one option to eliminate tumors in the liver.

High Purity Rare Earths

High purity rare earth oxides for use in research and development

A simple and economical procedure was developed to obtain high purity rare earths oxides. The raw material in the form of mixed rare earths carbonate is delivered after industrial separation of rare earths, thorium and uranium from Brazil' monazite. Using both ammonical precipitation and cationic ion exchange techniques, with EDTA solution as eluent, high purity rare earths oxides (99-99,9%) were obtained with impurity levels identical to those imported. The yield of this combined technique was reasonably high ≥ 70%. Molecular absorption spectrophotometry was used to monitor the rare earths content during the process and mass spectrometry to determine purity. Typical praseodymium oxide presents the following contaminants in micrograms per gram - Sc(18.20); Y (20.20); La (6.75); Ce (26.10); Nd (3.31); Sm (18.30); Eu (17.00); Gd (19.40); Tb (16.30); Dy (16.90), Ho(17.90); Er (18.40); Tm (16.90); Yb (17.60); Lu (17.70). Typical neodymium oxide presents the following contaminants in micrograms per gram - Sc(4.2); Y (1.40); La (7,75); Ce (6.21); Pr (5,31); Sm (12.3); Eu (11.2); Gd (10.4); Tb (15.3); Dy (6.92), Ho(7.49); Er (6.4); Tm (3.0); Yb (4.53); Lu (15.7).

High purity rare earths' acetate

Praseodymium acetate was prepared from praseodymium oxide Pr_6O_{11} ≥ 99.9%, treated in acetic acid medium. Sc(15); Y (15); La (5); Ce (20); Nd (2); Sm (15); Eu (14); Gd (17); Tb (15); Dy (14), Ho(13); Er (15); Tm (14); Yb (16); Lu (15).

Solubility behavior of rare earths with ammonium carbonate and ammonium carbonate plus ammonium hydroxide: Precipitation of their peroxicarbonates

The purpose here is to report the significant behavior of the rare earths when treated with ammonium carbonate and with a binary mixture of ammonium carbonate plus ammonium hydroxide. The carbonates of some rare earths are completely soluble in ammonium carbonate or in ammonium carbonate plus ammonium hydroxide, while others are only partially soluble and finally some are completely insoluble. Addition of hydrogen peroxide to the soluble complex rare earth carbonates results in the precipitation of a series of new compounds described as rare earth peroxicarbonates. The rare earths have a different precipitation behavior in the carbonateperoxide system. Some are completely and immediately precipitated, others are completely precipitated after an aging period, and some are not precipitated at all. These differing behavior opens up new possibilities in separation chemistry of rare earths. Sm, Gd, Dy, Y, Yb and Tm dissolve quickly and are completely soluble in ammonium carbonate. Ho, Eu and Tb are completely soluble in ammonium carbonate but dissolve slowly. La, Ce, Pr and Nd are only partially soluble in ammonium carbonate. While Ce, Pr, Nd, Sm, Eu and Dy are completely and easily soluble in the ammonium carbonate plus ammonium hydroxide mixture, La is only partially soluble and Tb is completely insoluble in the same mixture. Among the peroxicarbonates, La, Ce, Pr, Nd, Sm, Eu, Gd, Dy and Ho are quantitatively precipitated. The precipitation of the Er peroxicarbonate is quantitative, but after an aging period of 24 h. Y is not precipitated at all. The process is very easy, simple and economically attractive. Eventhough the process has been demonstrated on a bench scale, scale-up is considered to be feasible (Figure 14).

Figure 14. Assembly made to prepare high purity rare earth' oxides by ion exchange

Magnetic and Electric Materials

Significant progress has been made in R&D activities related to these materials over the past three years and consisted mainly of production of hydrogen processed magnetic and electric materials. Magnets and batteries have been produced and investigated and the results have been published in international journals. The microstructure and properties of magnetic materials based on Pr-Fe-Co-B alloy have been studied. Electric materials based on La-Al-Mg-Mn-Co-Ni alloys have also been studied and promising results were obtained. Batteries and magnets have been produced using the hydrogen decrepitation process and standard powder metallurgy route. Due to the extremely high prices of Dy and Co, alternate elements are being introduced in the alloys to overcome this problem.

In the last three years the main R&D activities were: (a) development of technologies and processes as well as management to mitigate environmental impact caused by solid wastes; (b) support efforts to increase energy efficiency, by designing components for fuel cells and porous burners for biogas. Besides, this group used green technologies to make use of debris (from civil construction) and wastes (from ornamental stones) to produce glass-silicate fibers known as e-glass, that is widely used as reinforcement in polymeric or metallic structures (Fig. 15).

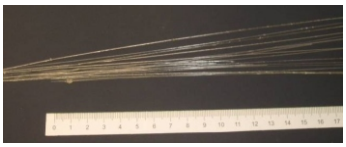

Figure 15. Glass fibers from SiO_2-NaO-CaO-B_2O_3-R_2O_3 glasses

The optimization of processes based on thermodynamic concepts derived from phase diagrams that enabled incorporation and inertization of galvanic solid wastes with heavy metals (up to 40wt%) in soda-lime-borosilicate glass. Based on these results, glasses with higher hydrolytic attack strength than commercial glasses were produced. High color frits with similar compositions were obtained for ceramic enamel. For crystalline glass ceramics, color shifts from green to brown with metallic brightness (as aventurine), has shown increased commercial application (Figure 16). In partnership with almost 27 galvanic/electroplating factories and the São Paulo State Institute for Technological Research (IPT/SP) a database of the volume of wastes generated from these activities in the eastern part of São Paulo was prepared. Based on this, technological options were provided to store, reduce and reuse galvanic mud produced in that region.

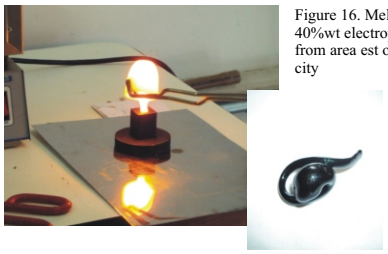

Figure 16. Melting glass with 40%wt electroplating waste from area est of São Paulo city

International environmental directives such as "Waste Electrical and Electronic Equipment" (WEEE) and "Restriction of Use of Certain Substances in Electrical and Electronic Equipment" (RhoS), that are operative in the European community (EU) and North America, were applied to evaluate Brazilian electro medical devices. These actions, without high cost processes, showed that Brazilian products are competitive. In the context of increased product upgrades and discard of electronic equipment, this group evaluated and developed technologies for re-qualifying, recovering and recycling e-waste from mainly, IPCs. To prevent discard of wastes in emerging technological areas this group is involved in inertization in a vitreous matrix of toxic metal nano-wastes produced from the use of nano-catalysts in direct ethanol polymeric fuel cells.

Other activities carried out by this group include: synthesis of materials like lanthanum chromite for applications in ceramic interconnectors; in lighting transmission from doped yttria and doped yttrium dissilicate for biogas burners; colloidal conformation involving rheology, such as tape casting and slip casting, to conform solid oxide fuel cell components; development of a replica method using natural fibers as template to produce porous ceramic membranes for use as mantles in biogas lighters. (Figure 17).

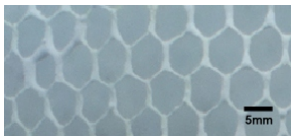

Figure 17. Sintered ceramic yttria based membrane for biogas burning

The development of high temperature glass matrix from BaO-SiO_2-Al_2O_3 for sealants has been studied. This composition is considered to have the right parameters in terms of mechanical strength and thermal expansion coefficient for use in solid oxide fuel cells.

A process based on mechanical alloying has been developed to enable direct low temperature sintering of nickel-zirconia (Ni-YSZ) cermets. The milled powder morphologies were pod-like or wafer-like, where the round fine ceramic particles - the pies were plated with metallic lamellae the pod. Alloying this powder with specific additives and oxygen partial pressures lead to the development of a new low-temperature consolidation process: Sintering by Activated Surface (SAS). Ni-YSZ plus Cu powders can be readily sintered to good densities by SAS rendering nano-sized constituents with good dispersion and pore structure (Fig. 18). The same process was also used for YSZ electrolyte to enable sintering around 1200°C.

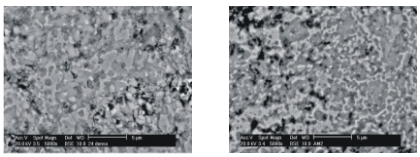

Figure 18. Sintered cermets: Cu-Ni-YSZ (left) and Cu-Mo-Ni-YSZ (righ)

The TG/DTA data coupled with mass spectrometric analysis validated the above mentioned approach suggesting that the process to dry reform methane can be optimised. The last result is the main contribution to state-of-art research.

High energy milling has been used to obtain nanocrystalline TiFe intermetallic compound by mechanically alloying the two elements in powder form (Figure 19). Powders were handled in an argon-filled glove box with automatic control of the humidity and oxygen contents. A PCT (pressure-composition-temperature) system was built to characterize hydriding/dehydriding behavior of hydrogen storage materials. The operation of the system was made entirely automatic by a PLC, solenoid valves, and electronic pressure as well as flow controllers. PCT curves can be measured in two modes: static (as a Sievert apparatus) and dynamic (hydrogen flow maintained constant).

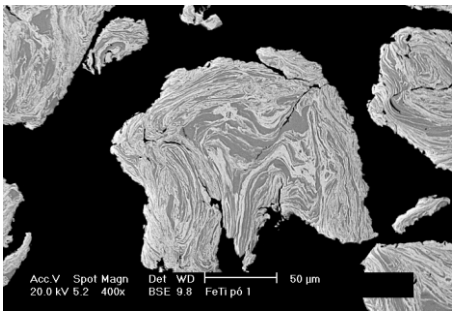

Figure 19. Partial mechanical alloying of a Ti+Fe mixture showing particles with lamellae microstructure (white and gray phases are Fe and Ti, respectively)

In the development of metallic components using powder metallurgy techniques, high speed steel powders with niobium were used. The main objective was to use of the high wear resistance of austenitic stainless steel in the manufacture of filters. Exploratory TIG welding was performed to increase the height of the filters (Figure 20 and 21).

Figure 20. TIG welding on stainless steel filters

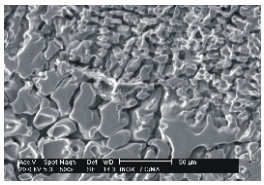

Figure 21. Interface of the weld metal and heat affected zone in filters (SEM)

High-pressure cell for neutron diffraction experiments

The high-pressure cell body consists of a zircaloy cylinder encapsulated in a carbon fiber composite and this device has innovative applications. Use of the high-pressure cell will permit neutron diffraction experiments of polycrystalline materials under high hydrostatic pressures to study “in situ”, high pressure phase crystal structure transformations, among other pressure induced transitions. This device, one of its kind, will be available to scientists in the field of neutron diffraction using the IPEN neutron diffractometer, which is also one of its kind in Brazil. Similar cells, also innovative, were developed by this group for high pressure x-ray diffraction and absorption studies, and were made available to users of the National Synchrotron Light Laboratory - LNLS / CNPq in Campinas.

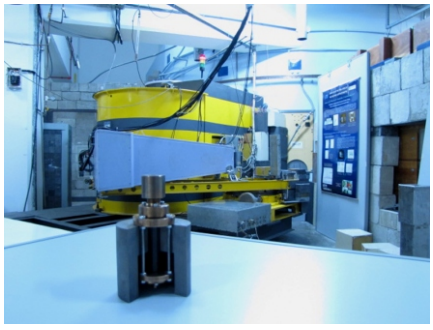

Figure 22. High-pressure cell (front) and the neutron diffractometer in the background

Standard Reference Materials for Powder Diffraction

The development of reference standard materials for calibration and determination of instrumental parameters of equipments used in diffraction (conventional x-rays, synchrotron and neutrons) is of paramount importance. The following standard high quality materials for diffraction were obtained: silicon (Si), yttria (Y_2O_3), lanthanum hexaboride (LaB_6), α-alumina (Al_2O_3), ceria (CeO_2), hydroxyapatite, silicon nitride and others. Other materials for SAXS, XAFS and for in situ measurements under high hydrostatic pressures are being prepared. The first samples have been sent to other Brazilian institutions and abroad for testing and the feedback has been encouraging.

Copper alloy wires for use in electrical transmission lines

Copper is a ductile metal that has high electrical and thermal conductivity. However, adequate mechanical properties are required for it to be used as power supply lines. Consequently, alloying elements are added to copper to improve its mechanical properties, without significantly altering its electrical conductivity. The objective of this project was to develop copper alloys for use as power transmission wire. The steps involved in the manufacture of copper wires were studied, starting with melting of copper and magnesium in an arc furnace, dilution of the melts in a resistance furnace and casting in a copper die. The billets were then forged and drawn into wires. The wires were characterized in terms of its mechanical properties and electric conductivity. The yield and the ultimate tensile strengths increased with increase in the alloying element content, while the electrical conductivity decreased to approximately 60% of IACS.

The Microscopy Laboratory of IPEN is well equipped, enabling examination and analysis of a variety of materials (ceramics, metals, polymers and composites) using multiple techniques. The scanning electron microscope (SEM) with a conventional tungsten filament has been used to observe particulate samples (fig. 23), fracture surfaces (fig. 24), dense polished and etched samples (fig. 25), glass microspheres sintered to different extent and bio-mimetic coatings on metals (fig. 26). The scanning electron microscope with a field emission gun (FEG-SEM) allows examination and analyses similar to that in a conventional SEM, but at higher resolution, as shown in fig. 27. Due to the high intensity of the beam in the FEG-SEM, it is possible to obtain x-ray maps of chemical constituents in samples. The transmission electron microscope (TEM) has been used extensively. Fig. 28 reveals the pores in a mesoporous silica. Thin foils of materials can be observed and the TEM allows determination of grain size, morphology, analysis of sub grain and precipitates, as well as EDS (energy dispersive spectroscopy) analysis of regions, or line scans, which reveals variation in concentration of different elements (Al, Si, Mn, Cu). High-resolution images can be obtained, and the crystal structure of specific regions can be determined, fig. 29.

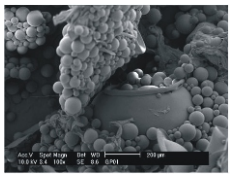

Figure 23. SEM micrograph of polymer microspheres

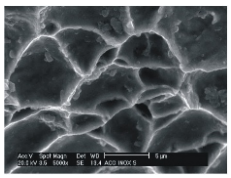

Figure 24. SEM micrograph of fracture surface on stainless steel

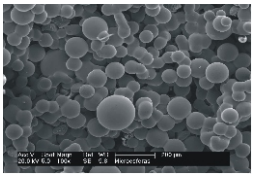

Figure 25. SEM micrograph of sintered glass spheres

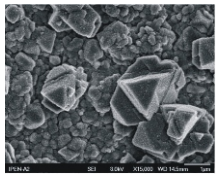

Figure 26. SEM micrograph of a bio-mimetic coating on metal

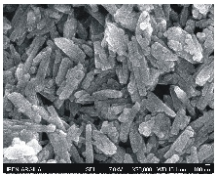

Figure 27. Image of Nanometric clays, obtained in the FEG-SEM

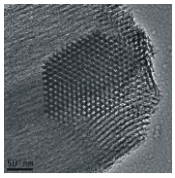

Figure 28. TEM of mesoporous silica

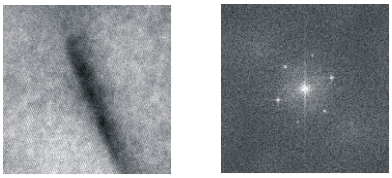

Figure 29. HTEM showing crystalline structures (left) and Fourier Transformed (FT) analysis (right) of the same field

Nanotechnology has been pointed as a high innovative technology allowing a deep and wide change in the materials production and application. The molecular design in an atomic scale is a new concept starting in technology that allows a new functionality of the matter. This leads to the control of the physical, optical, electronic, surface and magnetic properties and reactivity of the nanostructured functional materials. The nanotechnology is today one of the main points of the research activities, development and innovation in all of the industrialized countries. There are some nanotechnological products in the current market, but there's a trend to increase production in a short time. That new technology concept has been at development at IPEN, by the study of nanostructured functional materials. The following activities are in development:

Nanostructured coatings

Chromium carbide

Mechanically milled nanocrystalline feedstock powders of Cr_3C_2-Ni20Cr were used to develop thermally sprayed nanostructured coatings. These coatings were more uniform, exhibited higher hardness, high temperature erosion-oxidation resistance, increased fracture toughness and thermal stability compared to conventional coatings of the same materials.

Chromium dioxide

Thin film chromium dioxide coatings on steel substrates were prepared by MOCVD for increased high temperature oxidation resistance of the substrate. (Fig. 30)

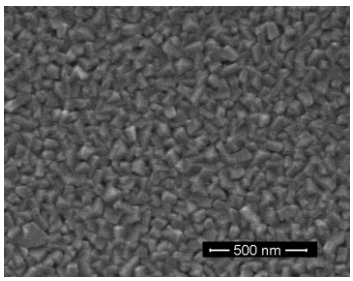

Figure 30. Surface of chromium dioxide thin film prepared by MOCVD

Titanium dioxide

Titanium dioxide (TiO_2) is an important commercial material and is used extensively in applications such as cosmetics, paint pigments, building materials, antibacterial surfaces, biomaterials and solar cells. Thin films of TiO_2, shown in Fig. 31, were grown under different conditions using the MOCVD technique.

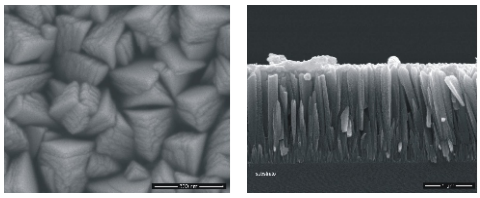

Figure 31. TiO_2 film grown at 500ºC on patterned Si. (a) surface; (b) cross-section

Indium Oxide nanoparticle and application

Indium oxide, a wide band gap (~3.6 eV) transparent semiconductor is of great interest for many device applications due to the unusual combination of high transparence in the visible region and high electrical conductivity. Current applications of indium oxide are in electro optic modulators, in the electronic field as window heater, electrochromic mirrors, solar cells, and flat-panel displays. Moreover, nanostructures based on indium oxide are promising device materials for chemical sensors and in the upcoming nanoelectronic building blocks. Indium oxide nanoparticles were synthesized by a surfactant-free room-temperature soft chemistry route. After thermal treatment of the gels at 400ºC indium oxide nanoparticles of 8 nm of average size were obtained. A small population of nanoparticles of 2.8 nm in size was evidenced by small-angle X-ray diffraction. The single-crystalline nature of the produced nanoparticles was confirmed by transmission electron microscopy. The synthesized material exhibits a weak and broad photoluminescence emission in the blue-UV region due to a quantum size effect.

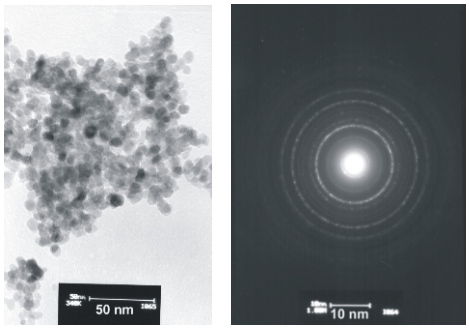

Figure 32. Bright-field TEM micrograph and selected area diffraction of In_2O_3 nanoparticles

Titanium dioxide nanostructured films: characterization and nanotechnological applications

Nanoscience and Nanotechnology is a scientific-technological field committed to understanding how the control of matter at the molecular level may lead to the development of new materials with unique and exclusive properties. Among these characteristics, the nanomaterials have got an extraordinarily high ratio of surface area to volume

and their mechanical and electrical properties are considerably improved. The numerous potential applications of nanomaterials have led researchers to consider them as the "philosopher's stone" of modern science that among the major challenges is the question of environmental sustainability. As solar energy is an abundant resource there, it is of great interest to find ways and means to collect this energy as to create an ecologically and healthy environment. Nanoporous and nanostructured films and surfaces have been successfully exploited for these spectacular effects. So a very promising material within nanotechnology applications for the use of solar energy is titanium dioxide nanostructured films which are able to absorb solar energy by converting it into chemical energy. Our studies seek mainly the improvement of the photocatalytic activity of titanium dioxide nanostructured films for the development of green technologies related to wastewater treatment and solar cells with high efficiency conversion of solar energy in the production of electricity.

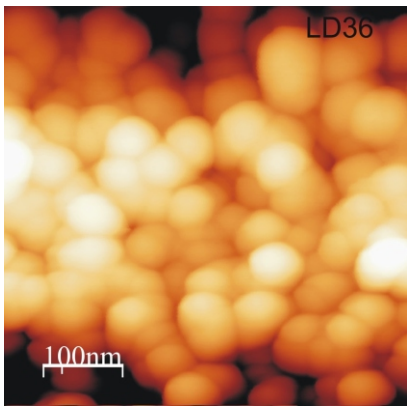

Figure 33. AFM image of nanostructured TiO_2 film demonstrating control of morphology in the molecular level

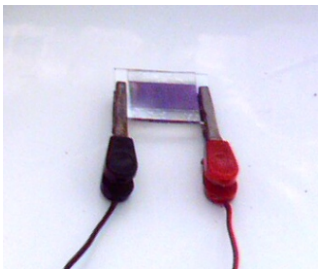

Figure 34. Biosolar cells with TiO_2 nanostructured films and natural dye

Electro-oxidation of ethanol using PtSnRh/C electrocatalysts prepared by an alcohol-reduction process

Pt/C, PtRh/C (90:10 and 50:50), (Pt:Sn 50:50) and PtSnRh/C (Pt:Sn:Rh 50:40:10) electrocatalysts were prepared in a single step (co-reduction of mixed metal ions) using ethylene glycol as solvent and reducing agent in the presence of Vulcan XC72. The X-ray diffractograms of Pt/C, PtRh/C, PtSn/C and PtSnRh/C electrocatalysts are shown in Fig. 35. All diffractograms showed a broad peak at about 25° that was associated with the Vulcan XC72 support material and four peaks at approximately 2 = 40°, 47°, 67°and 82°, which are associated with the (111), (200), (220) and (311) planes, respectively, of the face-centered cubic (fcc) structure characteristic of platinum and platinum alloys. In the diffractograms of PtSn/C and PtSnRh/C it was also observed two peaks at approximately 2θ = 34°and 52° that were identified as a SnO_2 phase. The (220) reflections of Pt(fcc) crystalline structure were used to calculate the average crystallite sizes using the Scherrer equation and the calculated values were in the range of 22.5 nm. It was observed that the (220) diffraction peak of PtRh/C (50:50) was dislocated to higher angle compared to Pt/C and PtRh/C (90:10) indicating an alloy formation between Pt and Rh. Similarly, the (220) diffraction peak of PtSnRh/C electrocatalyst was also dislocated to higher angle compared to PtSn/C electrocatalyst. TEM micrographs of PRh/C(90:10) (Fig. 36a), PtRh/C (50:50) (Fig. 36b), PtSn/C (Fig. 36c) and PtSnRh/C (50:40:10) (Fig. 36d) electrocatalysts showed a good distribution of the Pt particles on the carbon support with particle sizes of 3.0±1.0 nm, which is in agreement with XRD results.

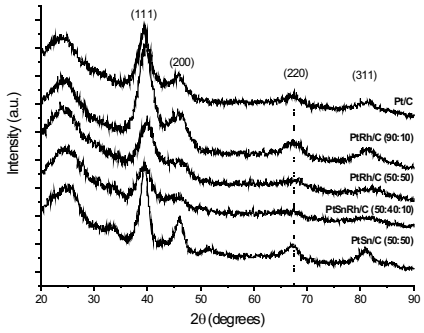

Figure 35. X-ray diffractograms of Pt/C, PtRh/C, PtSn/C and PtSnRh/C electrocatalysts

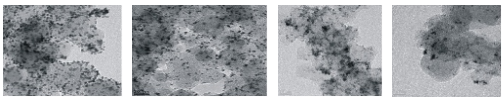

Figure 36. Transmission electron micrographs (20 nm) of PtRh/C (90:10) (fig 36a), PtRh/C (50:50) (fig 36b), PtSn/C (50:50) (fig 36c) and PtSnRh/C (50:40:10) (Fig 36d) electrocatalysts

Magnetite nanoparticles and magnetic carrier technology as adsorbent of metallic ions and dyes

Synthetic magnetite nanoparticles have been prepared by precipitation process of the Fe^{2+} and Fe^{3+} ions with a basic solution and from precipitation of Fe^{2+} ions and were subjected to heat treatment in water bath and microwave irradiation. Characterization studies were carried out for

various heating times and the two types of synthetic magnetite were compared. The techniques used were X-ray powder diffraction (DRX), transmission electronic microscopy (TEM), scanning electronic microscopy (SEM), thermogravimetric analysis (TGA), Fourier transform infrared spectroscopy (FTIR), differential scanning calorimetry (DSC) and magnetization curves (VSM). Fig. 37 shows the prepared magnetite nanoparticles from Fe^{2+} ions and subjected to microwave irradiation. They are good adsorbents of metallic ions and dyes and may be easily removed from wastewater using a magnet due to their magnetic properties. Synthetic magnetite nanoparticles have been studied as adsorbent of U ions from nitric solutions and have shown great perspective as an alternative adsorbent to conventional adsorbent.

The magnetite nanoparticles have been conjugated with adsorbent materials for obtaining magnetic carrier and its effect on enhancement adsorption capacity has been investigated. The technology of magnetic carrier for the wastewater treatment combines contaminant separation by sorption and magnetic recovery into a simple and compact process. Also called magnetic adsorbent it provides a simple way to remove contaminants from solutions under a wide range of chemical conditions. Adsorbents as chitosan, sugarcane bagasse and synthetic zeolite, from mineral coal fly ash, were combined with the magnetite nanoparticles for obtaining magnetic adsorbents. Characterization and adsorption studies of U and Mo ions, Reactive Orange 16, Indigo Carmine and Congo Red dyes and proteins were carried out. The performance of the magnetic adsorbents was investigated varying the pH, dose of adsorbent, agitation time and adsorption temperature using the batch system. The equilibrium data were analyzed by the Langmuir and Freundlich isotherm models. The magnetic adsorbent of chitosan presented the best results of adsorption of the U ions, and moreover showed that trypsin, BSA and collagen can be adsorbed. The Langmuir model was found to best describe the equilibrium isotherm data and the pseudo second-order model was found to explain the rapid kinetic of sorption. For all studied adsorption processes, the Gibbs free energy indicated the spontaneous nature. The magnetic zeolite exhibited a potential application in treatment of textile wastewater as an efficient and low cost adsorbent for dye removal. In 2008-2010, this research has produced three patents pending and one Master completed in 2010.

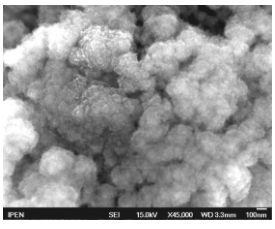

Figure 37. Magnetite nanoparticles prepared from Fe^{2+} ions and subjected to irradiation in a domestic microwave oven by Holland H

Preparation and characterization of smart magnetic hydrogels and its use for drug release

We have synthesized magnetic hydrogels based on chitosan that were successfully fabricated by chemically cross-linking of glutaraldehyde and $MnFe_2O_4$ nanoparticles (ca. 10-50 nm) to be used in biotechnology applications (drug release).
Those hydrogels were cured by two sources of energy γ-radiation (cobalt source with 3, 5, 10 KGy and 60 Watts UV-radiation lamp). For characterization, the hydrogels were dried until constant weight and analyzed by infrared spectra (IR), thermal analyses and UV absorption spectra The IR spectra of dried materials showed characteristic bands of chitosan, attributed to ν_{OH}= and ν_{NH} centered at 3446 cm^{-1}, Amide I band corresponding to $\nu_{C=O}$ vibration (1650 cm^{-1}) of acetyl groups in chitosan. The band Amide III at 1332 cm^{-1}, due to combination of NH deformation and the ν_{CN} stretching vibration and the band due to ν_{C-O} at 1089 cm^{-1}.The magnetic particles showed bands at ca. 600 and 400 cm^{-1} attributed to the stretching ν1 and ν2 from octahedral and tetrahedral sites of crystalline structure respectively. Thermal analyses (TGA/DTGA) showed three events of loss. Molecular absorption spectra in UV-vis showed large bands in visible line of spectra. All swelling behavior is plotted on the average of three trials. The cross-sectional SEM observation demonstrates that the $MnFe_2O_4$ nanoparticles were fairly uniformly distributed in the gel matrix.
The swelling kinetics and time dependent-swelling behaviors of chitosan/glutaraldehyde/ $MnFe_2O_4$ hydrogels was obtained in deionised water (pH 7) and serum solution.
Moreover, in vitro release data reveal that drug release profile of the resulting hydrogels is controllable by switching on or off mode of a given magnetic field. While applying magnetic fields to the magnetic hydrogels, the release rate of vitamin A of the hydrogels was considerably decreased as compared to those when the field was turned off, suggesting a close configuration of the hydrogels as a result of the aggregation of $MnFe_2O_4$ nanoparticles. Based on this on-&-off mechanism, the smart magnetic hydrogels based on the hydrogels ferrite hybrid composites can be potentially developed for application in novel drug delivery systems.

Development of luminescent and magnetic membranes based on chitosan and crosslinked with exudate of cashew

Natural polysaccharides such as chitosan in acidic medium, present the amine groups protonated, allowing ionic interactions between their cationic groups and anionic groups present in polysaccharides exudates. Covalent interactions and formation of imine groups (-C = N-), cannot be

disregarded. As a result of these kind of interactions membranes with good mechanical strength and able to function as drug-releasing, with no toxic agents in their formation are achieved.
The incorporation of manganese ferrite (Ni-Zn-Mn), a ceramic material with super paramagnetic behavior and β-diketonate complexes of rare earths, into the chitosan membranes, allow study the functionalization of the drug release matrix by the magnetic field and could follow the drug release monitoring the luminescence of the complex. The swelling of chitosan membranes crosslinked with exudate of cashew, shows that when the percentage of crosslinking increases, the swelling capacity of the membrane decrease.
The micrographs show the surface of chitosan membranes, enlarged 25 times. For membranes without crosslinking the surface appears smooth and without pores. The membranes with 1% and 3% of crosslinking present a crystalline structure and could be observed the pore formation. The membrane with 5% crosslinker has an amorphous structure with no crystallinity and pore.

Potential applications for the use of rare earth complexes and nanoparticles as luminescent biolabels

The ever growing interest in rare earth coordination compounds and materials with optical properties stems from applications in multidisciplinary fields such as nanosensors, materials for telecommunications, lighting devices, and luminescent probes for bioanalyses and live cell imaging and sensing. Most of these applications use the unique ability of the rare earth ions to emit well-defined narrow bands in different spectral ranges, from visible to near-infrared. Due to the low absorption cross-section of the f-f transitions, efficient population of the excited 4f states has to rely on energy transfer from the surroundings of the metal ion (antenna effect or luminescence sensitization). Another point desirable is the use of RE^{3+} ions with emission in the near-infrared (NIR) region reducing the interference from biological materials in the analyses.
At this point, special attention was given and reported to the preparation and characterization of rare earth coordination compounds and nanoparticles based on rare earth ions. RE^{3+} β-diketonate complexes with macrocyclic ligands, tetracycline, piroxican and carboxilate have been synthesized and characterized and are being used to mark hemoglobin S (sickle cells) *Leishmania* (tropical desease) and PSA (Prostate-specific antigen that is a protein produced by cells of the prostate gland. The PSA test measures the level of PSA in the blood). Several nanoparticles based on Nd^{3+}, Eu^{3+} and Tb^{3+} ions doped into the Y_2O_3 matrix, are also being synthesized and evaluated for labeling anti-oxLDL (anti-oxidized low density lipoproteins), one of the principal causes of cardiovascular diseases and responsible for around 30% of deaths worldwide. Information about structure and average grain size of these nanoparticles were obtained by x-ray diffraction (XRD), transmission electron micrograph (TEM) and infrared absorption spectroscopy.

Biolabeling with detection in the near-infrared luminescence based on $Y_2O_3:Nd^{3+}$ nanoparticles

Rare earth ions (RE^{3+}) are excellent luminescent probes for biological systems because their narrow emission bands are easily recognizable and well separated from the broad band fluorescence emission, which results in a high color purity of the emitted light. Moreover, applications in medical diagnosis make use of immunoassay detected by time-resolved luminescence in order to allow the separation of the RE^{3+} ions phosphorescence from the fluorescence of the biological samples. A number of important technological advances have been made by applying nanotechnology for biomolecular detection using luminescent RE^{3+} nanomaterials. Furthermore, nanoparticles are unique because their nanometer size gives rise to a high reactivity and beneficial physical properties (e.g. electrical, electrochemical, optical and magnetic) that are chemically inert.
The Nd^{3+} ion doped in Y_2O_3 matrix used in immunoassay can provided the benefit of being absorbed in visible and infrared irradiations (500 to 900 nm) with emission in the NIR region.

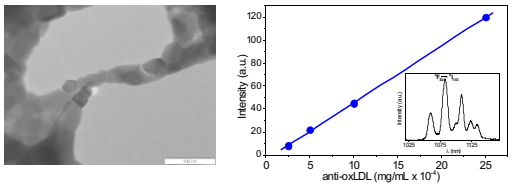

Figure 38. TEM image of Y_2O_3:2%Nd^{3+} nanoparticles and integrate emission intensity of $^4F_{3/2} \rightarrow {}^4I_{11/2}$ as function of functionalized nanoparticles bound to the LDL-antibody in the sensibilized plate with oxLDL-antigen. The insert figure shows the emission spectrum obtained from the sensitized well in the 96-plate containing the anti-oxLDL-labeled Y_2O_3:2%Nd^{3+} functionalized nanoparticles.

Preparation and photoluminescence properties of functionalized silica material incorporating europium complexes

The development of functionalized silica particles containing luminescent material has received special attention because of its biological applications such as optical markers *in vitro* and *in vivo*, clinical diagnosis and drug delivery.
New optical markers are still being developed, and rare earth materials are proposed as very attractive candidates. RE^{3+}-complexes containing carboxylate ligands are one the most largely investigated kind of coordination compounds due to higher thermal stability.
This work presents the development of a new process to obtain silica particles incorporating Eu^{3+}-complexes using APTES as a source of silica. The

synthesis was adapted from the literature, where the Y_2O_3:Eu^{3+} sample was used as label.
In summary, a kind of material incorporating Eu-BTC complexes has been prepared by a new method and has been characterized. The materials showed characteristic emission of Eu^{3+} ions. According to our results the most efficient luminescent system is the Eu-TMA-Si material, presenting the highest quantum efficiency $\eta = 27\%$. The outstanding aspect is clearly the transparency of the material based on modified silica, allowing the full detection of the Eu^{3+}-complex luminescence. Therefore, it is a promising candidate for molecular conjugation in clinical diagnosis.

Synthesis and characterization of SnO_2 and TiO_2 nanoparticles doped with lanthanide for biological labeling

Fluoroimmunoassay is an ultrasensitive technique for investigation of enzymes, antibodies, cells, hormones and others. The demand for highly sensitive systems brought the nanomaterials for biomedical and biotechnological field. Semiconductor nanocrystals (quantum dots) doped with lanthanide ions, when functionalized with biomolecules, can be used as luminescent biomarkers. Aiming this application, nanoparticles of titanium and tin mixed oxide doped with europium, terbium and neodymium have been synthesized and characterized. The synthesis was made by the co-precipitation method and characterized by SEM, IR, XRD, TGA and luminescence spectroscopy.

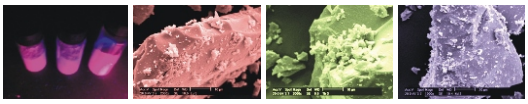

(a) (b) (c) (d)

Figure 39. (a) Nanoparticles of SnO_2/TiO_2:Eu^{3+}, (b) Mev SnO_2/TiO_2:Eu^{3+}, (c) Mev SnO_2/TiO_2:Tb^{3+} and (d) Mev SnO_2/TiO_2:Nd^{3+}

Europium Betha-Diketonate complexes with Tetracycline (Tc)

Luminescent materials containing trivalent rare earth (RE^{3+}) complexes with β-diketonate ligands have been intensively studied in recent years. The RE^{3+} compounds present characteristic narrow emission bands in the UV-Vis region, large Stokes shift and the antenna effect that enhance the overall quantum efficiency. As a result, these complexes have found wide applications as luminescent markers, photoluminescent sensors, electroluminescent devices, and multicolor display. In the field of biomarker these compounds have linked with biological parts.
At this point in time, four new complexes of europium β-diketonate with tetracycline as ligand were synthesized. IR spectra of the Eu(III) complexes show two strong absorption bands at ~1597 and ~1566 cm^{-1} attributed to ν_s(C=O) and ν_{as}(C=O) vibrational stretching modes, suggesting that the β-diketonate ligand acts as chelate ligand. SEM image showed particles rounded with grain size lower than 10 nm (Fig 40). The emission spectrum of europium complexes, in the solid state, recorded in the range of 420 to 720 nm at liquid nitrogen temperature, under excitation at β-diketonate transitions (~350 nm) is shown in Fig. 41. This emission spectrum exhibits characteristic narrow emission bands that are assigned to the $4f^6$-$4f^6$ transitions of Eu(III) ion, emanating from the emitting $^5D_0$ level to the ^7F_J (J = 0, 1, 2, or 4) levels, where the most intense corresponds to $^5D_0 \rightarrow {}^7F_2$ transition taking place around 613 nm. An important feature to be observed is the nonexistence of broaden bands arising from the β-diketonate centered transitions, indicating that intramolecular energy transfer from the β-diketonate ligands to the Eu(III) ion is operative.

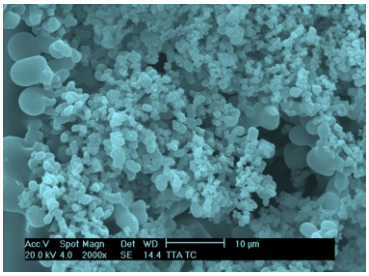

Figure 40. Scanning Electron Microscopy of the $Eu(TTA)_3(TC)_2$

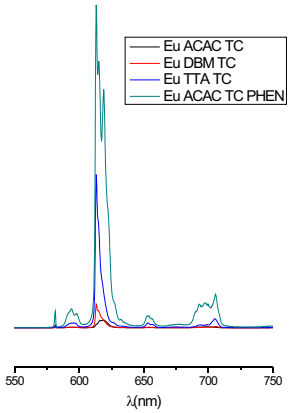

Figure 41. Emission Spectra of Eu(β-diketone)$_3$ TC_2

Development of nanobiomarkers for use in sickle cell anemia

Luminescent materials, such as the complex of rare earth, can be used as markers in cytology and immunology, being also used as luminescent biomarkers, once the development of these nanomaterials create new possibilities to many fields, particularly in diagnostic medicine. Besides, it establishes one kind of fluorescent probes, for which there are no equivalent organic molecules.

Due to its potential in market application, the objective of this work was to develop luminescent materials, allowing the use of these supermolecules of lanthanides as markers for the detection of Sickle Cell Disease (HbS). Six luminescent markers were developed based on rare earth compounds. The main methodology used for the detection of HbS was fluoroimunoassay, which is already used in investigation of enzymes, antibodies, cells, hormones, and so on. During this work, absorption spectrum in the infrared by Fourier's Transform (FTIR) was also used to detect the HbS.
The studied methods were applied for the diagnosis of this disease, which has genetic origin, very typical of the hemoglobin-pathology group and considered to be a public health problem in Brazil (ANVISA). When early diagnosed, Sickle Cell Disease (SCD) has a significant decrease in morbidity and mortality. Comparing the obtained results to the already known methodologies, it was possible to conclude that they are viable methods to detect HbS. Besides, when totally developed, these methods will contribute to the production of Sickle Cell Anemia's diagnostic, and they will have impact in São Paulo state public measures, as well as nationwide in Brazil.
We are extending our tools to validate a safe, sensitive and inexpensive methodology. Therefore, the Maldi-Toff method is being used in order to have a better understanding of the peptide profile on the target of biological materials. A database of most peptides present in the sickle cell disease will also be made in order to come up with the biomarking of HbS with Iodine-131 for comparative analysis of these methods.

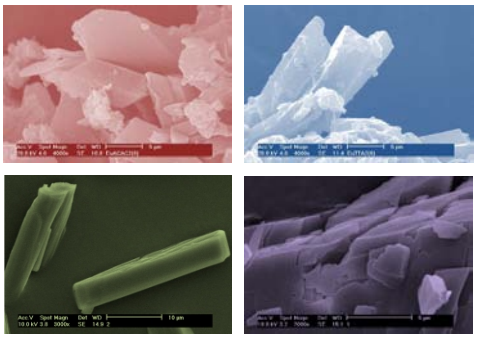

Figure 42. SEM of the Europium and terbium supermolecules

Persistent luminescent materials. Thermoluminescence and synchrotron radiation studies on the persistent luminescence of $Baal_2O_4:Eu^{2+},Dy^{3+}$

Since 1995, the research on persistent luminescence materials has increased substantially. This is due to the progress in the properties of these materials. Nowadays they can emit in the visible range up to 24+ hours, after ceasing the irradiation. Because of the long emitting time, these phosphors can be exploited commercially in emergency signs, road signalization, wall painting, watches, micro defect sensing, optoelectronics for image storage and detectors of high energy radiation. The persistent luminescence is not anymore just a scientific curiosity.
According to the literature, the $BaAl_2O_4(:Eu^{2+},R^{3+})$ materials are prepared via a solid state route, usually by heating $BaCO_3$ with Al_2O_3 (or their precursors) at elevated temperatures. However, low temperature routes as combustion and sol-gel syntheses are not uncommon. In the present work, the $BaAl_2O_4:Eu^{2+},Dy^{3+}$ materials were prepared with different synthesis methods and with different Eu^{2+} and Dy^{3+} concentrations. As usual, the combustion synthesis produces crystals with smaller size, evidently due to higher local temperature during the spontaneous explosion. Since the thermoluminescence analyses suggested the presence of one and three traps for the combustion and solid state prepared materials, respectively, the method of preparation has a significant effect on the defect structure of the materials. The mismatch between the band gap (E_g) value obtained from the synchrotron radiation excitation spectra and the DFT calculation was deduced to result from the covalent bonding in the $BaAl_2O_4$ host. The XANES spectroscopy showed a predominance of Eu^{3+} which can be present as a result of the *in situ* conditions of persistent luminescence during the X-ray irradiation. A systematic study of the effect of other R^{3+} co-dopants than Dy^{3+} is needed to a better understanding of the persistent luminescence mechanism of $BaAl_2O_4:Eu^{2+},Dy^{3+}$.

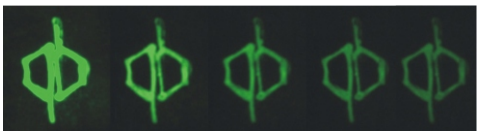

Figure 43. Afterglow of persistent material

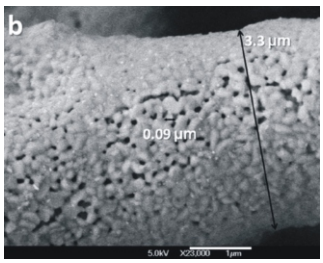

Figure 44. SEM Images of the $BaAl_2O_4:Eu^{2+},Dy^{3+}$ phosphors prepared by the combustion method

Luminescence-Tuneable multicolour PMMA films doped with Lanthanide B-Diketonate complexes

Interest in luminescent materials containing trivalent lanthanide ions (Ln^{3+}) as emitting centres has grown significantly in recent years. However, the Ln^{3+}-complexes generally present low thermal

stability, limited photostability and poor mechanical properties. Another parallel challenge is that most of these compounds are usually achieved as hydrates, consequently the luminescence intensity is suppressed due to the activation of non-radiative channels. In order to overcome simultaneously these deficiencies and improve the characteristics of light emission (*e.g.* quantum yield, lifetimes), Ln^{3+}-complexes have been incorporated into organic polymers, liquid crystals and sol-gel derived organic-inorganic hybrids. Polymers offer several advantages for the development of materials, such as: flexibility, versatility, optical quality and moderate processing conditions. By incorporating luminescent Ln^{3+}-complexes within the polymer matrix, the resulting product represents not only the sum of individual contributions of both organic and inorganic phases, but also novel properties for a new class of materials. In the present work, diaquatris(thenoyltrifluoroacetonate)-europium(III), $[Eu(tta)_3(H_2O)_2]$, ditriphenylphosphine oxide (thenoyltrifluoroacetonate)-europium(III), $[Eu(tta)_3(TPPO)_2]$, triaquatris(acetyl-acetonate)Terbium(III), $[Tb(acac)_3(H_2O)_3]$ and triphenylphosphine oxide (acetyl-acetonate)Terbium(III), $[Tb(acac)_3(TPPO)_2]$, complexes were co-doped into the PMMA polymer in order to obtain multicolor light-emitting devices due to their strong luminescence and relatively simple and inexpensive preparations.

λ_{exc} = 254

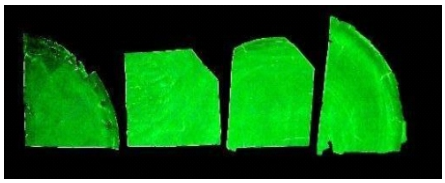

PMMA: x%$Tb(acxac)_3(H_2O)_2$

Figure 45. Samples of PMMA films under and without UV irradiation excitation

Nanomaterials for organic light emitting devices

Complexes containing Rare Earth ions are of great interest in the manufacture of electroluminescent devices as organic light emitting devices (OLED). OLEDs are regarded as the next generation flexible flat panel display technology and a new platform for low-cost illumination source. These devices, using rare earth trivalent ions (TR^{3+}) as emitting centers, show high luminescence with extremely fine spectral bands due to structure of its levels of energy, a long lifetime and high quantum efficiency. The preparation was made of rare earth β-diketonate complexes (tta = tenoyltrifluoroacetonate and acac = acetylacetonate) (Tb^{3+}, Eu^{3+} e Gd^{3+}) contend crown ether macrocyclic ligand (DB18C6 = dibenzo18crown6). The thermal analyses of the $Eu(tta)_3(DB18C6)_2$ and $Tb(acac)_3(DB18C6)_2$ and morphology are important in the manufacture of OLED devices using PVD technique. This Physical Vapor Deposition used in this work have been done with lab thin film which belongs to Departamento de Física da Pontifícia Universidade Católica do Rio de Janeiro - PUC - Rio and Lab-*f* from Chemistry Institute-São Paulo University.

Formation of chitosan-cashew gun hydrogel with UV radiation

Chitin, obtained from lobster, shrimp and crab shell waste, is the second most abundant polysaccharide found in nature. In the 21st century, chitin and its derivative (chitosan) face new opportunities to contribute to functional materials and environmentally friendly materials as to meet the diverse needs of today society because of their nontoxic, biodegradable, biocompatible, antibacterial, etc.
UV Radiation processed chitosan cashew gun hydrogels have been observed to be suitable for producing transparent, flexible, mechanically strong, biocompatible, effective and economical hydrogel. No additives were used and different formulations containing chitosan and cashew gun selected from combinations, also with agar, were used to make the hydrogels. Chitosan formulations containing the cashew gun and agar show significantly different pre-gel viscosities behavior. By increasing the concentration of agar in the formulation, it converts the sheet gel to paste gel useful for filling wound cavities. For characterization, the hydrogels were dried until constant weight and analyzed by infrared spectra (IR) thermal analyses, scanning electron microscopy and UV absorption spectra. The results indicate that the pre-irradiation network structure of the formulation plays an important role in properties of the irradiated gel dressing. Scanning electron micrographs show highly porous structure of the gel. To observe swelling response of the chitosan/Cashew gum hydrogels when exposed to different pH conditions, the hydrogels were emerged until equilibrium in an aqueous medium of pH 2, 4, 7 and 9 at 25°C. The hydrogels presented higher swelling content in acid medium. The hydrogels will be observed to be useful in treating burns, non-healing ulcers of diabetes, drug controlled deliver and other external wounds.

Synthesis, characterization and cytotoxicity of polymeric hydrogels for use to immobilization and drug release on Leishmaniasis treatment

Hydrogels were obtained with poly(N-vinyl-2-pyrrolidone) (PVP), poly(vinyl alcohol) (PVAl) and poly(ethylene glycol) (PEG). The process of obtaining was: 1) irradiation process using ^{60}Co gamma source, 2) Crystallizing process of freezing/thawing thermal cycles, and 3) crosslink by chemical reaction with citric acid in chloride acid as catalyses. The hydrogels obtained were characterized by Thermogravimetry Analysis (TGA), differential scanning calorimetric (DSC), gel content, swelling, scanning electronic microscopy (SEM), Fourier transform infrared spectroscopy (FTIR) and cytotoxicity by neutral red test.
Insertion of nanoclays in PVAl/PVP hydrogels performs distinct characteristics and the presence of PEG is essential to the membranes properties. Cytotoxicity behavior was similar to negative control curves indicating that matrices have no toxicity when formulated with laponite nanoclay. Higher thermal stability was observed in membranes obtained by gamma and chemical process was showed in displacement of PVAl decomposition temperature associated to higher crosslink stability in presence of nanocompound studied. Glucantime immobilization was done in membranes that showed higher crosslinking obtained by different processes. Drug delivery was observed in period of 24 hours and similar results were achieved. The different processes of PVAl/PVP hydrogels have performed different release kinetics. The characteristics of homogeneity, integrity, no cytotoxicity and swelling of the systemized membranes are qualities of suitable hydrogels for drug delivery and biomedical applications.

Development of sulfonated multifunctional fluoroelastomer based on nanocomposites

Nanomaterials are new research areas that have been attracting a lot of attention due to their potential applications in several areas such as: electronics, optics, catalysis, ceramics, magnetic data storage, and polymer nanocomposites. These nanomaterials are incorporated in polymer matrices which makes it possible to improve the performance and physical-chemical properties for the modified material. These researches reveal that it is necessary to incorporate a small quantity of inorganic material in order to obtain a polymer with better properties than the original, for example: nanoparticles of POSS and clay incorporated in a polymer matrix are used to improve mechanical and barrier properties. The objective of this project is the synthesis and characterization of ion exchange membranes, from nanostructered fluoroelastomer. This process of nanostructering will be realized by nanoparticle of POSS and clay incorporated in the polymer matrix.

Development of HMSPP with nanoparticles of silver with biocide activity

HMSPP is a long chain branched PP as a result of radiation modification of PP in presence of acetylene monomer to promote the grafting of long chain branches. This study started in the doctorate project of Washington L Oliani, based on the study of microgel structures in HMSPP and silver inclusion.
Among the wide variety of plastics, polypropylene of high melt strength (HMSPP) offers overall balanced properties (mechanical, thermal, chemical, drawability, etc. Characterization of thermal stability and degradation processes at temperatures useful ranges of HMSPP-Ag compounds with different formulations and processing conditions was carried out by differential scanning calorimetry (DSC). Presence of silver nanoparticles also slightly improves thermal stability of HMSPP-Ag compounds thus enabling easy processing; this could be done to the interaction between polypropylene chains and surfactant-coated silver nanoparticles. These interactions lead to a decrease in motion of polymer chains and also, they act as nucleating sites for crystallization. XRD diffraction patterns of HMSPP-Ag compounds show presence of silver since the main diffraction peak of silver is located at typical 2η angle. Future tests will be done for biocide activity evaluation.

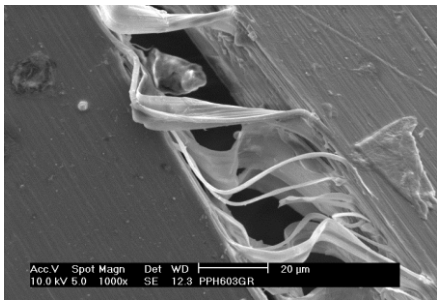

Figure 46. PP nanostrucure

Development of thermoplastic starch films and packing products from renewable sources

Starch is a natural, renewable, biodegradable polysaccharide produced by many plants as a storage polymer. It usually has two major components, a largely linear amylose of molecular weight between one thousand and one million and amylopectin, having the same backbone as amylose but with a myriad of α-(1→6)-linked branch points. The most commercially important starch for the development of thermoplastic starch is corn in most countries, however in tropical countries starch from tapioca appear to be a much more interesting source. Native starch occurs in the form of discrete and partially crystalline microscopic granules that are held together by an extended micellar network of associated molecules. A small amount of water is always associated with this structure, therefore the use of this bound water as expansion agent is an opportunity to developed foam with very low impact to the environment.
Starch is not truly thermoplastic as most synthetic polymers. However, it can be melted and made to flow at high temperatures under pressure and shear. If the mechanical shear becomes too high, then starch will degrade to form products with low molecular weight. Addition of water or other plasticizers enables starch to flow under milder conditions and reduces degradation considerably. However, the thermomechanical stability is strongly reduced by the addition of plasticizers. This project has developed a mixture of starch and nanoparticles for production of active and smart films and it was also developed very resistant packing with the addition of natural fibers.

Figure 48. Foams of Starch and Sugar cane bagasse for packing application

New hydrogels and silicone matrix as polymeric biomaterials for applications in the heath and cosmetic industry

New hydrogel dressings were developed from PVP and PVA. Hydrogels were synthetized by radiation induced crosslinking and freeze and thawing method, without the use of extra chemicals, usually very toxic. Multiple drugs were incorporated to these hydrogels and due to its characteristics, special formulations were developed. For instance:

- Hydrogels with Assai oil as powerful radical scavenger for anti-aging properties;
- Hydrogels with resveratrol (from grapes) as powerful radical scavenger for anti-aging properties;
- Hydrogels with algae extract for new skin formation and skin quality;
- Hydrogel with nanosilver incorporation to avoid contamination of wounds.

Silicone matrix were also used to encapsulate essence oils with repellency activity.

Figure 49. Silicone matrix with natural oils for repellency

Microwave and ionizing radiation assisted degradation of rubber and heavy oil

The saturated polymer systems (rubber) and butyl rubber (BR) used in the manufacture of tires and rubber chlorobutyl and bromobutyl used to make inner-air in the tires, electric wires and cables and has high resistance to the action of oxygen, ozone, solar radiation and bacteria, thus contaminate the environment for long periods of time. The re-use of these polymers also reduces the emission of substances give (aliphatic) in the atmosphere. The objective is to develop processes of controlled degradation (devulcanization) of butyl rubber and halobutyl rubbers (chlorine and bromine) using radiation of Co source. The development of combined methodologies as thermal degradation and ionizing radiation produce recycled material with characterized properties to be applied in new formulations.
Several types of petroleum hydrocracking and hydrotreating processes can benefit from microwave technique. It has recently been studied all over the world to identify (qualitatively and quantitatively) and define the mechanism of microwave-material interaction. Rubbers devulcanization is one of the main stream of this line. The application of this process in our country is a very recent field and has been studied as a new tool in materials processing for rubber devulcanization, which uses high temperatures and shear and also for heavy oil degradation as well as desulfurization of oil and diesel. The knowledge of this technology is important to begin the development process in industrial scale and consequently in reducing the environmental pollution caused by these kinds of residues.
Microwaves are a form of electromagnetic energy in the frequency band from 300MHz to 300GHz (not ionizing radiation). Industrial microwave processing is usually accomplished at a frequency of 2.45GHz (which corresponds to a wavelength of 12.24cm) to avoid interference with telecommunication and cellular phone frequencies. Microwave processing offers numerous advantages in relation to conventional heating methods (convection or conduction), where the material surface heats first and then the heat moves inward. One of the most important characteristics is saving energy, because the material absorbs microwaves readily (the heat is generated from the inner parts to the surface of the material) reducing the processing time. Also the selective energy absorption allows heating in specific points of the material. This process is environmentally clean because it reduces pollutant emission. Finally, the microwave heating requires no appreciable amount of time to effect temperature changes such as conventional methods and when the microwave device is turned off the effect of these electromagnetic waves are instantaneously stopped.

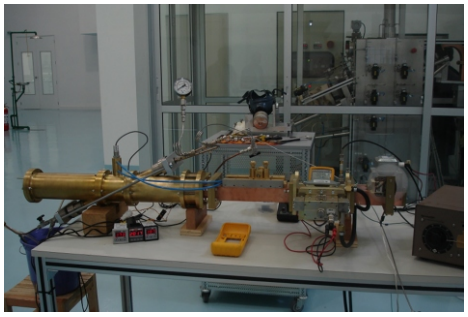

Figure 50. Microwave system

Development of nanohybrid materials and shrinkage evaluation

Dental filling materials used to repair decayed tooth structure are dental amalgam and composite materials based on acrylics. Photo-activated composites started to be used in the 60's, and are nowadays widely applied for dental restorative procedures. Polymerization of composite filling is considered to be an important factor in achieving longevity of the restorative treatment. Contraction induces certain amount of stress, which is transferred to surrounding dental structures (dentine and enamel).
The objective of the Phd work of Luiza M.P. Campos, oriented by Dr. Duclerc F. Parra, is the study of the dimensional changes in tooth and resin, produced by light-induced polymerization of dental composite filling. The first part in the study of shrinkage of different formulations was done with evaluation of thermo-mechanical analysis (TMA). The second part of the project was conducted in the University of Porto-Portugal using Digital Holography (DH) and ESPI. Both techniques present some characteristics that make them well adapted to this study; a high resolution can be achieved in non-contact displacement field measurements with small objects. All the preparations were placed in a digital holography or ESPI set up to obtain the holographic recordings. A blue led lamp (420nm - 480nm) is used to induce composite polymerization, and the real time deformation during resin cure was recorded. Experimental data was post processed for the deformation assessment. The study won the price Francisco Degni in the Scientific Forum of the CIOSP Congress-SP - Brazil and was presented at International Congress of ADA - Orlando, USA in 2010.

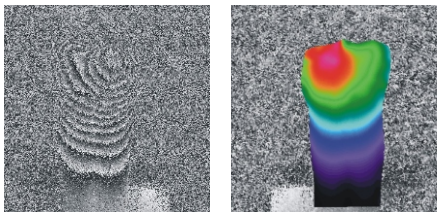

Figure 51. Toth deformation by digital holography

Materials and Nanotechnology

Program Team

Research Staff

Dr. Ademar Benevolo Lugao; Dr. Almir Oliveira Neto; Dr. Ana Helena de Almeida Bressiani; Dr. Ana Lúcia Exner Godoy; Dr. Armando G. Padial; Dr. Arnaldo H Paes de Andrade; Dr. Carlos Alberto da Silva Queiroz; Dr. Christina Aparecida Leao Guedes de Oliveira Forbicini; Dr. Cláudio José da Rocha; Dr. Chieko Yamagata; Dr. Cristiano Stefano Mucsi; Dr. Denise Alves Fungaro; Dr. Dolores Ribeiro Ricci Lazar; Dr. Duclerc Fernandes Parra; Dr. Eguiberto Galego; Dr. Eliana Navarro Muccillo; Dr. Emília Satoshi Miyamaro Seo; Dr. Estevam Vitorio Spinace; Dr. Fatima Maria Sequeira de Carvalho; Dr. Hélio Ferreto; Dr. Hidetoshi Takiishi; Dr. Isolda Costa; Dr. Ivana Conti Consentino; Dr. Jesualdo Luiz Rossi; Dr. Jorge Moreira Vaz; Dr. José Carlos Bressiani; Dr. José Fernando Correia Braga; Dr. José Roberto Matinelli; Dr. Lalgudi V. Ramanathan; Dr. Luis Antonio Gênova; Dr. Luiz Galego Martinez; Dr. Luzinete Pereira Barbosa; Dr. Maria Aparecida Faustino Pires; Dr. Maria Claudia Franca da Cunha Felinto; Dr. Marilene Moreli Serna; Dr. Marina Fuser Pillis; Dr. Mauricio David Martim das Neves; Dr. Mitiko Yamaura; Dr. Nelson Batista de Lima; Dr. Olandir V. Correa; Dr. Raquel de Morais Lobo; Dr. Reginaldo Muccillo; Dr. Ricardo Mendes Leal Neto; Dr. Rubens Nunes de Faria Jr.; Dr. Ruth Luqueze Camilo; Dr. Sonia Regina Homem de Mello-Castanho; Dr. Stela M.C.Fernandes; Dr. Sumair Gouveia de Araújo; Dr. Valter Ussui; Dr. Walter Kenji; MSc. Cecílio A. da Cunha; MSc. Francisco José Breda; MSc. Fredner Leitão; MSc. Lia Maria Carloti Zarperon; MSc. Luis Carlos Elias da Silva; MSc. Oswaldo Julio Junior; MSc. Vanderlei Ferreira; MSc. Yone Vidotto Franca; MSc. Yvone Vidotto França; Tech. Antonio Carlos Alberto Beraldo; Tech. Celso Vieira de Morais; Tech. Dileusa Alves da Silva Galassi; Tech. Eleosmar Gasparin; Tech. Eliel Domingos de Oliveira; Tech. Glauson A. F. Machado; Tech. Jenedite Souza Nascimento; Tech. Joana Domingos de Andrade; Tech. Judit C. da Silva; Tech. Marcelo Oliveira; Tech. Marco Andreolli; Tech. Mariqano Castagnet; Tech. Nelson Rodrigues Bueno; Tech. Nildemar Aparecido Messias Ferreira; Tech. Olandir Vercino Correia; Tech. Pedro Pinto de Freitas; Tech. Rene Ramos de Oliveira; Elizabete dos Santos; José Carlos Depintor; Mara Alcântara; Marlene F.P. Marcelino; Rui Marques de Lima; Sandra Cunha.

Graduate Students

Alan Andrade dos Santos; Alexander Rodrigo Arakaki; Amanda Abati Aguiar; Amanda Pongeluppe Gualberto Yamamura; Ana Carolina Ribeiro; Antonio Carlos da Silva; Antonio de Sant'Ana Galvão; Bruno Ferreira Antunes da Silva; Carola Gomez Agreda; Cecilio Alvares da Cunha; Charles de Miranda Christe; Claudia Akemi Kodaira Goes; Danilo F. Marin; Débora Christina Salum; Douglas Will Leite; Edison Bessa Gibelli; Edney Deschauer Rejowski; Edvaldo Roberto de Souza; Elen Gonçalves dos Santos; Eleni Cristina Kairalla; Eliner Affonso Ferreira; Elizabeth C. Carvalho; Emanuelle Zangerolame Santos; Eraldo Cordeiro Barros Filho; Eurico Felix Pieretti; Everton Bonturim; Fernanda Carvalho dos Santos; Francisco Carlos Cione; Gabriel Souza Galdino; Gilberto de Oliveira Moraes; Guilherme Wolf Lebrão; Heloísa Augusto Zen; Henrique Perez; Heveline Vieira; Jacinete Lima dos Santos; Joao Roberto do Carmo; Jose Helio Duvaizem; Jose Mario Ferreira Junior; José Roberto Moura; José Silva de Sousa; Juliana Pereira de Souza; Juliano da Silva Ignácio; Julio Cesar Serafim Casini; Kai Jiang; Kalan Bastos Violin; Karina Avelino da Silva; Karolina Pereira dos Santos Tonello; Klauss Engelmann; Leandro Augusto Pidone; Leandro Cesar Pereira Gomes Safra; Liana Key Okada Nakamura; Luis Claudio Aranha; Luiz Alberto Tavares Pereira; Luiz Fernando Grespan Setz; Luiza Mello de Paiva Campos; Marcelo Luis Ramos Coelho; Maria Cely Freitas Dias; Maria José Oliveira Alves; Mariano Castagnet; Maviael Jose da Silva; Mayra Dancini Gonçalves; Natalia Naime; Newton Koodi Terada Horimouti; Olavo Rodrigues de Oliveira; Oscar Luiz Ferreira Junior; Patricia Brissi Santos; Patrícia Ponce; Paula Pinheiro Paganini; Pedro Lima Forster; Rafael Henrique Lazzari Garcia; Rafael Morgado Batista; Rebeca Gomes dos Santos; Reinaldo Azevedo Vargas; Renata Hage Amaral; Ricardo Rodrigues Dias; Roberta Momesso; Robson Lopes Grosso; Rodrigo Mendes Mesquita; Rogerio Albuquerque Marques; Rosele Correia de Lima Yamaguti; Sandra Regina Scagliusi; Shirley Leite dos Reis; Silas Cardoso dos Santos; Silvio Andre de Lima Pereira; Silvio Luiz Ventavele da Silva; Suelanny Carvalho da Silva; Tadeu Noveli Cantarin; Talita Filier Fontes; Tamiye Simone Goia; Tatiane Cristina Porfírio; Teofilo Mendes Neto; Thatiana Goncalves Diegues; Washington L Oliani; Wilma Jasinski Wicher.

Undergraduate Students

Ana Holanda Sousa Silva; Andréia Navarro; Camila Pinheiro de Souza; Carolina da Silva Fernandes; Danielle Faria da Silva; Gabriel de Souza Hachisu; Gustavo Varca; Helber Holland; Katia Cristina Nunes; Lucas Narcizo de Moura; Michele Brandalise; Natasha Tercilia Barberi Cruz; Tamires F. Oliveira; Taynara Alves dos Santos; Thelma Antunes Rodrigues Kovacs.

Co-Workers

Dr. Ana Valéria Santos de Lourenço; Dr. Adriana Napoleão Geraldes; Dr. Ana Maria Segadães; Dr. Angelo Fernando Padilha; Dr. Antonio Carlos da Silva; Dr. Antônio Carlos de Oliveira Sobrinho; Dr. Antonio Carlos Ferreira Junior; Dr. Ariston da Silva Melo Junior; Dr. Armando Cirilo de Souza; Dr. Armando Guilherme Fernandes Padial; Dr. Benjamin Teixeira Dourado; Dr. Carla Costa Guimarães; Dr. Celia Regina Tomachuk dos Santos Catuogn; Dr. Christiane Ribeiro; Dr. Claudia

Program Team

Akemi Kodaira Goes; Dr. C. M. Garcia; Dr. Doris Maribel Escriba Villanueva; Dr. Douglas Gouvêa; Dr. Edson Souza de Jesus Filho; Dr. Edilson Rosa Barbosa de Jesus; Dr. Eduarda Maria Soares de Carvalho Tomas; Dr. Eduardo Caetano Camilo de Souza; Dr. Eduardo Milton Sanchez; Dr. Elki Cristina de Souza; Dr. Elson Longo; Dr. Eneida Graça Guilherme; Dr. Ercules Epaminondas de Souza Teotônio; Dr. Érica Caproni; Dr. Everson do Prado Banczek; Dr. E. Djurado; Dr. E. Traversa; Dr. Fabio de Camargo; Dr. Felipe Antunes Santos; Dr. Felipe de Oliveira; Dr. Flávio M. Vichi; Dr. Francisco Ambrósio Filho; Dr. Francisco Carlos Ceoni; Dr. Frank Ferrer Sene; Dr. Geise Ribeiro; Dr. Gilberto Vitor Zaia; Dr. Gonçalo Siqueira; Dr. Guilherme Wolf Lebrão; Dr. Hamilton Perez Soares Corrêa; Dr. Hermi Felinto de Brito; Dr. Hiro Goto; Dr. I. T. Weber; Dr. Jivaldo do Rosário Matos; Dr. João Alberto Osso; Dr. Jorma Hölsä; Dr. José Carlos dos Santos; Dr. José Octávio Armani Paschoal; Dr. José Roberto Rogero; Dr. José Serafin Moya Corral; Dr. J. F. Q. Rey; Dr. Leandro César Pereira Gomes Safra; Dr. Lucas C. V. Rodrigues; Dr. Lucio Salgado; Dr. Luís Cláudio Aranha; Dr. Luis Filipe Pedroso Cardoso de Lima; Dr. Luiz Alberto Tavares Pereira; Dr. Luiz Antonio de Oliveira Nunes; Dr. Luiz Filipe C. P. Lima; Dr. Magnus A. Gidlund; Dr. Marcio Willians Duarte Mendes; Dr. Marco Antônio Colosio; Dr. Marcos Gonzales Fernandes; Dr. Marcos Tadeu D'Azeredo Orlando; Dr. Maria Elena Leyva González; Dr. Matheus Chianca Ferreira; Dr. Maysa Terada; Dr. Mika Lastusaari; Dr. M. Malkamaki; Dr. M. A. C. Berton; Dr. M. C. Steil; Dr. Nelson Marques da Silva; Dr. Oscar M. L. Malta; Dr. Rejane Aparecida Nogueira; Dr. Renata Bressane; Dr. Renato Altobelli Antunes; Dr. Risoma Chaves; Dr. Roberval Stefani; Dr. Rodrigo Moreno; Dr. Rogério Albuquerque Marques; Dr. Roseli Correa de Lima; Dr. R. A. Rocha; Dr. R. F. Jardim; Dr. Sergio Allegrini Junior; Dr. Sergio Luis de Assis; Dr. Sidney Jose Lima Ribeiro; Dr. Solange de Sousa; Dr. Stela Maria C. Fernandes; Dr. Taneli Laamanen; Dr. Thais Da Silva Santos; Dr. Thomaz Augusto Guisar Restivo; Dr. Vania Trombini Hernandes; Dr. Waldemar; Alfredo Monteiro; Dr. Wilson Acchar; MSc. Maria Edileuza F. Brito; MSc. Sizue Rogero.

Honor Mentions and Awards

The Brazilian Society of Science in Laboratory Animals (SBCAL) honored the work "Influence of ionizing radiation on well being of animals producing anti ophidic serum", realized by Nanci do Nascimento, Miriam C. Guarnieri, Pedro C.L. Oliveira and Roberto Rogero, during the XI Brazilian Congress of Science in Laboratory Animals and the II Forum of Ethic Committee on Animal Use.